JCTC Journal of Chemical Theory and Computation

Article

Cite This: J. Chem. Theory Comput. 2018, 14, 4590−4599

pubs.acs.org/JCTC

Wavefunction-like Correlation Model for Use in Hybrid Density Functionals

Timothy C. Wiles and Frederick R. Manby*

Centre for Computational Chemistry, School of Chemistry, University of Bristol, Bristol BS8 1TS, United Kingdom

Supporting Information

ABSTRACT: We present Unsöld-W12 (UW12), an approximation to the correlation energy of molecules that is an explicit functional of the single-particle reduced-density matrix. The approximation resembles one part of modern explicitly correlated second-order Møller−Plesset (MP2) theory and is intended as an alternative to MP2 in double-hybrid exchange−correlation functionals. Orbital optimization with UW12 is straightforward, and the UW12 energy is evaluated without a double summation over unoccupied orbitals, leading to a faster basis-set convergence than is seen in double-hybrid functionals. We suggest a one-parameter hybrid exchange−correlation functional XCH-BLYP-UW12. XCH-BLYP-UW12 is similar to double-hybrid functionals, but contains UW12 correlation instead of MP2 correlation. We find that XCH-BLYP-UW12 is more accurate than the existing double-hybrid functional B2-PLYP for small-molecule main-group reaction barrier heights and has roughly the same accuracy as the existing hybrid functional B3LYP for atomization energies.

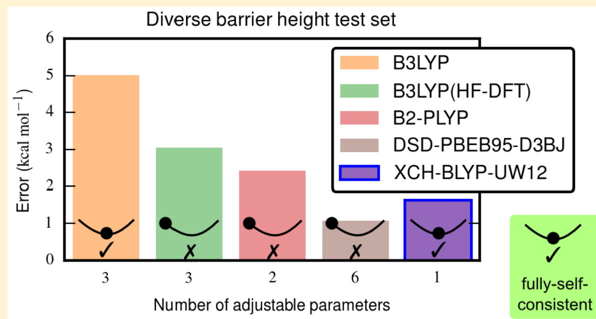

I. INTRODUCTION

In hybrid density-functional theory (DFT), the exchange−correlation energy is expressed as a sum of semilocal[1] (DFT) and nonlocal (nl) parts

$$E_{xc} = a_{xc}^{DFT} E_{xc}^{DFT} + a_{xc}^{nl} E_{xc}^{nl} \tag{1}$$

where E_{xc}^{DFT} is a functional of the electron density[2] $\rho(\mathbf{x})$, whereas E_{xc}^{nl} is a functional of the single-particle reduced-density matrix (1-RDM)

$$\rho(\mathbf{x}|\mathbf{x}') = \sum_i \phi_i^*(\mathbf{x})\, \phi_i(\mathbf{x}') \tag{2}$$

where $\{\phi_i\}$ are occupied Kohn−Sham spin−orbitals (we use spin−orbitals throughout unless otherwise stated). Typically, the nonlocal part, E_{xc}^{nl}, is chosen to be the Hartree−Fock exchange energy given by

$$E_x^{HF} = -\frac{1}{2}\sum_\sigma \int d\mathbf{r}_1 \int d\mathbf{r}_2 \frac{|\rho^\sigma(\mathbf{r}_1|\mathbf{r}_2)|^2}{|\mathbf{r}_1 - \mathbf{r}_2|} \tag{3}$$

where $\sigma = \uparrow,\downarrow$ is a spin variable.

For instance, the B3LYP hybrid functional[3] is defined as

$$E_{xc}^{B3LYP} = (1 - a_x^{HF} - a_x^{B88})E_x^S + a_x^{HF}E_x^{HF} + a_x^{B88}E_x^{B88} + (1 - a_c^{LYP})E_c^{VWN} + a_c^{LYP}E_c^{LYP} \tag{4}$$

where E_x^S is the Slater−Dirac exchange functional, E_c^{VWN} is the Vosko−Wilk−Nusair (VWN) correlation functional,[4] E_c^{LYP} is the Lee−Yang−Parr (LYP) correlation functional,[5] and E_x^{B88} is Becke's 1988 exchange functional.[6] The adjustable parameters $a_x^{HF}, a_x^{B88}, a_c^{LYP}$ = 0.20,0.72,0.81 were fit[7] to the 56 atomization energies, 42 ionization potentials, 8 proton affinities, and the 10 first-row total atomic energies of ref 8. Despite being widely used throughout chemistry, B3LYP systematically underestimates reaction barrier heights due to an incomplete cancellation of the self-interaction error.[9]

The B-HH-LYP[10] hybrid functional

$$E_{xc}^{B\text{-}HH\text{-}LYP} = \frac{1}{2}E_x^{B88} + \frac{1}{2}E_x^{HF} + E_c^{LYP} \tag{5}$$

is more accurate than B3LYP for reaction barrier heights, but systematically underestimates atomization energies. This phenomenon has been attributed[11] to the larger fraction of exact exchange in B-HH-LYP (a_x^{HF} = 0.50) than in B3LYP (a_x^{HF} = 0.20). Is it possible to make a functional that is accurate for both reaction barrier heights and atomization energies?[12,13]

For some time, there have been efforts to overcome these problems by adding additional nonlocal terms to the energy expression. In double-hybrid DFT, the nonlocal part of the exchange−correlation energy is expressed as

$$E_{xc}^{nl} = a_x^{HF}E_x^{HF} + a_c^{virt}E_c^{virt} \tag{6}$$

where E_c^{virt} is a nonlocal model of the correlation energy that depends on the unoccupied (virtual) orbitals and their eigenvalues $\{\phi_a, \epsilon_a\}$, in addition to the occupied orbitals and eigenvalues $\{\phi_i, \epsilon_i\}$. Addition of E_c^{virt} leads to a so-called "fifth-rung" functional.[9] In 2006, Grimme[14] proposed choosing E_c^{virt}

Received: April 9, 2018
Published: August 6, 2018

to be the second-order Møller–Plesset (MP2) correlation energy E_c^{PT2}, building on the earlier development of Görling–Levy perturbation theory[15,16] and related composite methods by Truhlar.[17,18]

The resulting B2-PLYP double-hybrid functional is defined as[14]

$$E_{xc}^{B2\text{-}PLYP} = (1 - a_x^{HF})E_x^{B88} + a_x^{HF}E_x^{HF} + (1 - a_c)E_c^{LYP} + a_cE_c^{PT2} \tag{7}$$

where the empirical parameters a_x^{HF}, a_c = 0.53, 0.27 are optimized for the heats of formation of the G2/97 set. Similarly, the 1DH-BLYP[11] and the (more recent) LS1-DH[19] double-hybrid functionals are defined as

$$E_{xc}^{1DH\text{-}BLYP} = (1 - \lambda)E_x^{B88} + \lambda E_x^{HF} + (1 - \lambda^2)E_c^{LYP} + \lambda^2 E_c^{PT2} \tag{8}$$

$$E_{xc}^{LS1\text{-}DH} = (1 - \lambda)E_x^{B88} + \lambda E_x^{HF} + (1 - \lambda^3)E_c^{LYP} + \lambda^3 E_c^{PT2} \tag{9}$$

where in each case λ is an adjustable parameter between 0 and 1. To evaluate eqs 7, 8, and 9, the Kohn–Sham orbitals $\{\phi_p\}$ are first optimized[20] in a self-consistent manner ignoring the MP2 correlation energy E_c^{PT2} term. The E_c^{PT2} energy is then calculated using the resulting orbitals and eigenvalues $\{\phi_p,\epsilon_p\}$.

In 2008, Zhang et al.[21] proposed an alternative methodology. They used the orbitals and eigenvalues from a B3LYP calculation to calculate the E_c^{PT2}, E_x^{HF}, and E_{xc}^{DFT} components of the energy and constructed the XYG3 functional

$$E_{xc}^{XYG3} = (1 - a_x^{HF} - a_x^{S})E_x^{B88} + (1 - a_c^{PT2})E_c^{LYP} + a_x^{S}E_x^{S} + a_x^{HF}E_x^{HF} + a_c^{PT2}E_c^{PT2} \tag{10}$$

where the empirical parameters a_x^{HF} = 0.8033, a_x^{S} = −0.0140, and a_c^{PT2} = 0.3211 are optimized for the heats of formation of the G3/99 set. One advantage of XYG3 over B2-PLYP is that XYG3 correctly models the integer discontinuity for systems with non-integer charge.[22]

Limitations of Existing Hybrid and Double-Hybrid Functionals. Even the most recent conventional hybrid functionals suffer from self-interaction error,[23] meaning they are surpassed in accuracy by double-hybrid functionals in almost all cases (particularly barrier heights and nonbonded interactions). After an exhaustive study of both hybrid and double-hybrid density functionals, the authors of ref 24 recommend that double hybrids should be used whenever possible. However, implementing the MP2 energy expression efficiently is not a trivial task, so double-hybrid functionals are not available in many popular electronic structure codes. They also concede that hybrid functionals have been shown to outperform double-hybrid functionals in transition-metal chemistry[24−26]—and that this is an ongoing area of research. It is somewhat unsatisfying that the electron density is not optimized using the full energy expression in the methods mentioned so far. This can lead to unphysical behavior when spin-unrestricted calculations are performed.[27−29] Not only that, but the calculation of gradients and other first-order response properties is made more involved by the fact that the energy is not minimized (stationary) with respect to orbital rotations.

It should be mentioned that orbital-optimized double-hybrids have recently (since 2013) been developed to address this issue. The orbital optimization is not trivial to implement but leads to a better description of electron affinities, reaction barrier heights, and radical bond dissociation.[30−33] We hope to compare UW12 hybrids with orbital-optimized double hybrids in the future.

Other disadvantages to using conventional MP2 include the explicit summation over the unoccupied Kohn–Sham orbitals $\{\phi_a\}$ in eq 11. This gives double-hybrid functionals a slower basis-set convergence than hybrid functionals.[9]

Our search should therefore be for new correlation models that can achieve chemical accuracy (when included in a hybrid density functional), have only a few parameters, are easy to implement into existing electronic structure codes, can be orbital-optimized, and have fast convergence with respect to basis and low computation scaling.

In this work we investigate the possibility of adding terms to E_{xc}^{nl} that have wavefunction character (are similar to E_c^{PT2}) but which depend only on *occupied* Kohn–Sham orbitals $\{\phi_i\}$. More specifically, we will seek expressions that are explicit functionals of the 1-RDM $\rho(\mathbf{x}|\mathbf{x}')$. The total energy can thus be minimized with respect to $\rho(\mathbf{x}|\mathbf{x}')$ in the usual Kohn–Sham manner.

II. THEORY

Unsöld-W12 Correlation Energy. The second-order Møller–Plesset (MP2) correlation energy for a system (neglecting contributions from singly excited determinants[34]) is given by

$$E_c^{PT2} = -\frac{1}{2}\sum_{ijab}\frac{\langle ij|r_{12}^{-1}|\overline{ab}\rangle\langle ab|r_{12}^{-1}|ij\rangle}{\epsilon_a + \epsilon_b - \epsilon_i - \epsilon_j} \tag{11}$$

where $|i\rangle,|j\rangle \equiv \phi_i,\phi_j$ are occupied Kohn–Sham spin–orbitals, and $|a\rangle,|b\rangle \equiv \phi_a,\phi_b$ are unoccupied (virtual) spin–orbitals in an infinite single-particle basis. In principle, the set $\{\phi_a\}$ is infinite. However, in practical implementations of E_c^{PT2}, finite basis sets are used. The ket $|\overline{pq}\rangle$ is defined as

$$|\overline{pq}\rangle = |pq\rangle - |qp\rangle \tag{12}$$

In the Unsöld approximation the denominator is approximated as a single-characteristic energy gap Δ to give

$$E_c^{U} = -\frac{1}{2}\frac{1}{\Delta}\sum_{ijab}\langle ij|r_{12}^{-1}|\overline{ab}\rangle\langle ab|r_{12}^{-1}|ij\rangle \tag{13}$$

The model implicitly expresses the amplitudes for double excitations in the form

$$T_{ab}^{ij} \approx -\frac{1}{\Delta}\langle ij|r_{12}^{-1}|\overline{ab}\rangle \tag{14}$$

which, *prima facie*, is a terrible approximation. But without changing the structure of the theory, we can formulate models of the form

$$T_{ab}^{ij} \approx \langle ij|w_{12}|\overline{ab}\rangle \tag{15}$$

where w_{12} is a two-electron operator to be determined. We arrive at the Unsöld-W12 (UW12) correlation energy E_c^{UW12}

$$E_c^{UW12} = \frac{1}{2}\sum_{ijab}\langle ij|w_{12}|\overline{ab}\rangle\langle ab|r_{12}^{-1}|ij\rangle \tag{16}$$

Note that E_c^{UW12} is linear in the operator w_{12}, which we refer to as the "geminal" operator.

DOI: 10.1021/acs.jctc.8b00337
J. Chem. Theory Comput. 2018, 14, 4590−4599

Removing the Summation over Unoccupied Orbitals. In eq 16, it appears that calculating E_c^{UW12} requires summing over the (infinite set of) unoccupied orbitals $\{\phi_a\}$. We now show that E_c^{UW12} can be expressed in terms of only the (finite set of) occupied orbitals $\{\phi_i\}$. First recognize that

$$\sum_{ab} |\overline{ab}\rangle\langle ab| = \sum_{pq} |\overline{pq}\rangle\langle pq| + \sum_{ij} |\overline{ij}\rangle\langle ij| - \sum_{ip} |\overline{ip}\rangle\langle ip| - \sum_{ip} |\overline{pi}\rangle\langle pi| \quad (17)$$

is an exact identity, where $\{\phi_p\}$ is the (infinite) orthonormal set of all Kohn–Sham orbitals. Now recognize that the operator $\sum_p |p\rangle\langle p|$ is the unit operator in the (infinite) space of single-particle wavefunctions. Substituting eq 17 into eq 16, we arrive at

$$E_c^{\mathrm{UW12}} = E_{c,2el}^{\mathrm{UW12}} + E_{c,4el}^{\mathrm{UW12}} + E_{c,3el}^{\mathrm{UW12}} \quad (18)$$

where

$$E_{c,2el}^{\mathrm{UW12}} = \frac{1}{2}\sum_{ijpq} \langle ij|w_{12}|\overline{pq}\rangle\langle pq|r_{12}^{-1}|ij\rangle = \frac{1}{2}\sum_{ij} \langle \overline{ij}|w_{12}r_{12}^{-1}|ij\rangle \quad (19)$$

$$E_{c,3el}^{\mathrm{UW12}} = -\sum_{ijkp} \langle ij|w_{12}|\overline{kq}\rangle\langle kq|r_{12}^{-1}|ij\rangle = -\sum_{ijk} \langle \overline{ij}k|w_{12}r_{23}^{-1}|kji\rangle \quad (20)$$

$$E_{c,4el}^{\mathrm{UW12}} = \frac{1}{2}\sum_{ijkl} \langle ij|w_{12}|\overline{kl}\rangle\langle kl|r_{12}^{-1}|ij\rangle \quad (21)$$

Note that this is an exact relation and is made possible by the structure of the model in eq 16. Such a completeness relation is not possible in conventional MP2 theory (eq 11) due to the energy denominator $1/(\epsilon_a + \epsilon_b - \epsilon_i - \epsilon_j)$.

We can also write the components of E_c^{UW12} as explicit functionals of the 1-RDM:

$$E_{c,2el}^{\mathrm{UW12}} = \int d\mathbf{x}_1 \int d\mathbf{x}_2\, w_{12} r_{12}^{-1} \Gamma_{12|12}^{(2)} \quad (22)$$

$$E_{c,3el}^{\mathrm{UW12}} = -2\int d\mathbf{x}_1 \int d\mathbf{x}_2 \int d\mathbf{x}_3\, w_{12} r_{23}^{-1} \rho_{3|1} \Gamma_{12|32}^{(2)} \quad (23)$$

$$E_{c,4el}^{\mathrm{UW12}} = \int d\mathbf{x}_1 \int d\mathbf{x}_2 \int d\mathbf{x}_3 \int d\mathbf{x}_4\, w_{12} r_{34}^{-1} \rho_{3|1} \rho_{4|2} \Gamma_{12|34}^{(2)} \quad (24)$$

where the two-particle reduced-density matrix (2-RDM) is defined as

$$\Gamma_{12|34}^{(2)} = \frac{1}{2!}\begin{vmatrix} \rho_{1|3} & \rho_{1|4} \\ \rho_{2|3} & \rho_{2|4} \end{vmatrix} \quad (25)$$

and $\rho_{1|2} \equiv \rho(\mathbf{x}_1|\mathbf{x}_2)$.

Note that eq 20 contains three-electron integrals

$$\langle pqr|w_{12}r_{23}^{-1}|stu\rangle = \int d\mathbf{x}_1 \int d\mathbf{x}_2 \int d\mathbf{x}_3\, \phi_p^*(\mathbf{x}_1)\, \phi_q^*(\mathbf{x}_2)\, \phi_r^*(\mathbf{x}_3) w_{12} r_{23}^{-1} \phi_s(\mathbf{x}_1)\, \phi_t(\mathbf{x}_2)\, \phi_u(\mathbf{x}_3) \quad (26)$$

These can be calculated efficiently using grids, as outlined in the Appendix. In the Appendix, we show that the scaling for evaluating the Fock matrix using such grids is N^4 (where N is the size of the system).

Relationship to MP2-F12. In explicitly correlated second-order Møller–Plesset theory (MP2-F12), the linear term in the Hylleraas functional is given by[35]

$$E_c^{\mathrm{MP2-F12}} = \frac{1}{2}\sum_{ij\tilde{a}\tilde{b}} T_{\tilde{a}\tilde{b}}^{ij} \langle \tilde{a}\tilde{b}|r_{12}^{-1}|ij\rangle + \frac{1}{2}\sum_{ijkl} T_{kl}^{ij} \langle kl|f_{12}\left[\sum_{ab} |ab\rangle\langle ab| - \sum_{\tilde{a}\tilde{b}} |\tilde{a}\tilde{b}\rangle\langle \tilde{a}\tilde{b}|\right] r_{12}^{-1}|ij\rangle \quad (27)$$

where the indices $\tilde{a}\tilde{b}$ run over the (finite) set $\{\phi_{\tilde{a}}\}$ of all unoccupied orbitals in the given atomic orbital basis, and the indices ab run over the (infinite) set $\{\phi_a\}$ of all unoccupied orbitals in a complete single-particle basis. Consider the case where the atomic orbital basis is minimal, such that the set $\{\phi_{\tilde{a}}\}$ is empty. The expression then becomes

$$E_c^{\mathrm{MP2-F12}} = \frac{1}{2}\sum_{ijklab} T_{kl}^{ij} \langle kl|f_{12}|ab\rangle\langle ab|r_{12}^{-1}|ij\rangle \quad (28)$$

If we set the MP2-F12 occupied–occupied amplitudes to be

$$T_{kl}^{ij} = -(\delta_{ik}\delta_{jl} - \delta_{il}\delta_{jk}) \quad (29)$$

and the geminal $f_{12} = -w_{12}$; then eq 28 reduces to the UW12 correlation energy (eq 16). It is worth noting that in the F12 literature the idea of using just the linear part (or V-term) of the second-order Hylleraas functional has been investigated before[36,37] but was generally discarded as not being sufficiently accurate in the context highly converged wavefunction-based correlation methods.

MP2 Correlation Energy as a Laplace Transform. The MP2 correlation energy (defined in eq 11) can also be written as a Laplace transform[38]

$$E_c^{\mathrm{PT2}} = \int_0^\infty d\tau\, E_c(\tau) \quad (30)$$

where

$$E_c(\tau) = -\frac{1}{2}\sum_{ijab} e^{-\tau(\epsilon_a+\epsilon_b-\epsilon_i-\epsilon_j)} \langle ij|r_{12}^{-1}|\overline{ab}\rangle\langle ab|r_{12}^{-1}|ij\rangle \quad (31)$$

$$= -\frac{1}{2}\sum_{ijab} \langle ij|e^{-F_1\tau} e^{-F_2\tau} r_{12}^{-1} e^{F_1\tau} e^{F_2\tau}|\overline{ab}\rangle\langle ab|r_{12}^{-1}|ij\rangle \quad (32)$$

and F_1 (F_2) is the Fock operator that acts on electron 1 (electron 2). If we set the geminal operator to be

$$w_{12} = -\int_0^\infty d\tau\, e^{-F_1\tau}\, e^{-F_2\tau} r_{12}^{-1} e^{F_1\tau}\, e^{F_2\tau} \quad (33)$$

then the Unsöld-W12 correlation energy (eq 16) is equivalent to the MP2 correlation energy (eq 11). The challenge regarding Unsöld-W12 now reduces to finding a simple form for the operator w_{12} that does not depend on the system, but that still captures the physics of the problem.

Choosing the Geminal Operator w_{12}. Motivated by the r_{12} methods of explictly correlated electronic structure theory,[39,40,42] we now choose the operator w_{12} in eq 16 to be a function of the distance r_{12} between the two electrons

$$w_{12} = w^{s_{12}}(r_{12}) \quad (34)$$

DOI: 10.1021/acs.jctc.8b00337
J. Chem. Theory Comput. 2018, 14, 4590–4599

where $s_{12} = \delta_{\sigma_1\sigma_2}$ is the total spin of the two electrons (s_{12} = 0,1). Note that E_c^{UW12} is invariant to adding a constant c to $w^s(r_{12})$.

We can choose $w^s(r_{12})$ to correctly model the correlation at any length scale. Inspired by the work of Ten-no,[41] we choose $w^s(r_{12})$ to be a Slater function in the interelectron coordinate r_{12}

$$w^{s_{12}}(r_{12}) = -\frac{1}{2(s_{12}+1)} r_c e^{-r_{12}/r_c} \tag{35}$$

where r_c is a characteristic length scale for electron correlation.

Unsöld-W12 Hybrid Functionals. If we replace E_c^{PT2} with E_c^{UW12} in eq 8, and fix[42] the parameter $\lambda = 1/2$, we can define a new hybrid functional XCH-BLYP-UW12:

$$E_{xc}^{XCH-BLYP-UW12} = \frac{1}{2}E_x^{B88} + \frac{1}{2}E_x^{HF} + \frac{3}{4}E_c^{LYP} + \frac{1}{4}E_c^{UW12,r_c} \tag{36}$$

$$= E_{xc}^{B-HH-LYP} - \frac{1}{4}E_c^{LYP} + \frac{1}{4}E_c^{UW12,r_c} \tag{37}$$

The XCH-BLYP-UW12 functional contains a single adjustable parameter r_c, which both represents the length scale for the correlation hole and also scales the Unsöld correlation energy. We refer to XCH-BLYP-UW12 as a hybrid functional (as opposed to a double-hybrid functional) since it can be evaluated without an explicit summation over the unoccupied Kohn–Sham orbitals. We use the prefix XCH (exchange-and-correlation hybrid) because the functional contains nonlocal correlation as well as nonlocal exchange. Conventional hybrids such as B3LYP contain nonlocal exchange but only local correlation.

III. IMPLEMENTATION

Evaluating the UW12 Correlation Energy. The geminal $w^s(r_{12})$ is expressed as a sum of Gaussians

$$w^s(r_{12}) \approx w_{GTG}^s(r_{12}) = \sum_{\gamma} c_{s\gamma} e^{-\gamma r_{12}^2} \tag{38}$$

where the coefficients $c_{s\gamma}$ (given in the Supporting Information) are chosen to minimize the error

$$\Delta_{GTG}^s = \int_0^\infty dr_{12}\, [w_{GTG}^s(r_{12}) - w^s(r_{12})]^2 \tag{39}$$

according to the procedure outlined in ref 41.

We evaluate the three-electron integrals in eq 26 through a quadrature in the electron coordinate that couples the two operators together, as proposed by Boys and Handy[43] and independently re-discovered by Ten-no.[44] Thus, we compute the integral as

$$\langle ijk|w_{12}r_{23}^{-1}|lmn\rangle = s_{jm}\int d\mathbf{r}_2\, \phi_j^*(\mathbf{r}_2)\, \phi_m(\mathbf{r}_2)\langle i|w^{s_{il}}(\mathbf{r}-\mathbf{r}_2)|l\rangle\langle k|v(\mathbf{r}-\mathbf{r}_2)|n\rangle \tag{40}$$

where $s_{pq} = \delta_{\sigma_p\sigma_q}$, and $v(\mathbf{r}-\mathbf{r}_2) = 1/|\mathbf{r}-\mathbf{r}_2|$. The integral over $\mathbf{r}_2$ is then performed numerically using the SG-1 quadrature grid.[45]

The elements of the Fock matrix $F_{\alpha\beta}^\sigma = [\partial E_c^{UW12}/\partial D_{\alpha\beta}^\sigma + \partial E_c^{UW12}/\partial D_{\beta\alpha}^\sigma]/2$ are also calculated (see the Appendix), where $D_{\alpha\beta}^\sigma$ is an element of the Kohn–Sham density matrix in the atomic-orbital basis $\alpha(\mathbf{r})$, such that

$$\rho^\sigma(\mathbf{r}|\mathbf{r}') = \sum_{\alpha\beta} \alpha(\mathbf{r}) D_{\alpha\beta}^\sigma \beta(\mathbf{r}') \tag{41}$$

The energy expression can then minimized with respect to $\rho(\mathbf{x}|\mathbf{x}')$ using a self-consistent-field procedure.

A first inspection of eq 21 suggests that calculating the Fock matrix contribution $\partial E_{c,4el}^{UW12}/\partial D_{\beta\alpha}^\sigma$ scales formally as N^5 where N is the size of the system. However, in the Appendix we show that (using the same grid method used in eq 40) one may evaluate the Fock matrix in a computational time that formally scales as N^4. This is the same formal scaling as density-fitted Hartree–Fock exchange.

Aside: Laplace Transform MP2. It should be noted that Laplace-transform MP2 methods—in which the integral in eq 30 is approximated with a finite set of points in τ-space—also scale formally as N^4 (although they still suffer from the same slow basis-set convergence as standard MP2). This favorable computational scaling comes with the trade-off that one can only evaluate the opposite-spin $E_{c,s=0}^{PT2}$ component of E_c^{PT2}. Double-hybrid functionals which make use of a Laplace transform to evaluate E_c^{PT2} are hence referred to as spin-opposite-scaled double hybrids, and such methods rely on the E_c^{DFT} term to provide the correlation energy between same-spin electrons. Recent examples include DOD-PBEB95-D3BJ,[46] PWPB95,[47] XYGJ-OS,[48] and B2-OS3LYP.[49]

An advantage of UW12 is that we can evaluate both the same-spin $E_{c,s=1}^{UW12}$ and opposite-spin $E_{c,s=0}^{UW12}$ components in N^4 time. This means UW12 hybrids can be applied in systems where spin-opposite-scaled double hybrids (e.g., DOD-PBEB95-D3BJ) are not as accurate as conventional double hybrids (e.g., DSD-PBEB95-D3BJ).[9,46] In addition, the range dependence and spin dependence of the geminal $w^s(r_{12})$ in UW12 leads to the attractive possibility of using different length scales for the same-spin and opposite-spin correlation energy components: reflecting the fact that same-spin (opposite-spin) correlation is more important at long range (short range).[46]

IV. COMPUTATIONAL DETAILS

The UW12 correlation energy expression and the XCH-BLYP-UW12 functional were implemented in the electronic structure program entos.[50]

We use the Dunning aug-cc-pV(X+d)Z basis sets.[51−55] The B2-PLYP and DSD-PBEB95 calculations were performed with frozen-core MP2 unless otherwise stated.[56] All the electrons (both valence and core) were correlated in the XCH-BLYP-UW12 calculations. Energies of singlet molecules and atoms were calculated with the spin-restricted Kohn–Sham formalism, and energies of other molecules and atoms were calculated with the spin-unrestricted formalism. B2-PLYP and DSD-PBEB95 values were calculated in Molpro.[57,58] All other values were calculated in entos unless otherwise stated. For entos calculations, the Def2-SVP-JKFIT density-fitting basis set[59,60] was used. Density-fitting was not used for the Molpro calculations.

V. RESULTS AND DISCUSSION

Atomization Energies and Barrier Heights. We seek a method that can correctly estimate both atomization energies and barrier heights. Following the procedure of ref 11, we optimize the value of the single parameter r_c in XCH-BLYP-UW12 on the AE6 (atomization energies) and BH6 (barrier heights) test sets.[61] All the calculations for the AE6 and BH6

DOI: 10.1021/acs.jctc.8b00337
J. Chem. Theory Comput. 2018, 14, 4590−4599

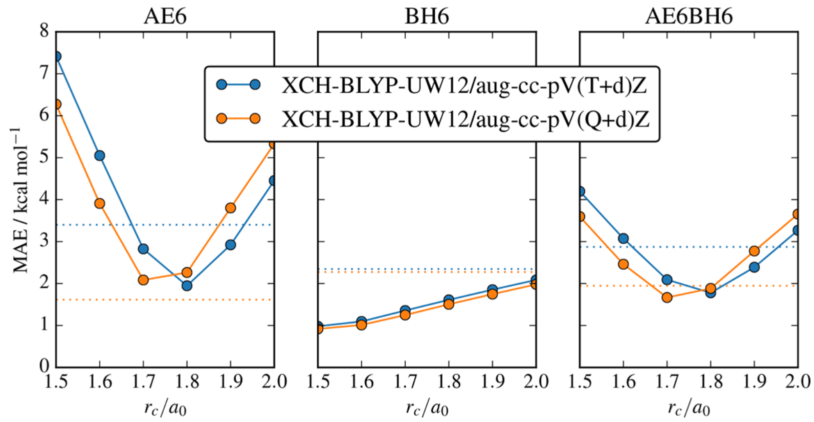

Figure 1. Mean absolute errors (MAEs) for the AE6 (far left), BH6 (center), and combined AE6+BH6 (far right) test sets[61] as functions of the parameter r_c for the single-parameter UW12 hybrid functional XCH-BLYP-UW12. In this plot, the XCH-BLYP-UW12 results use B3LYP orbitals rather than using full self-consistency. The horizontal dotted lines show the MAE for the existing two-parameter double-hybrid functional B2-PLYP.[14]

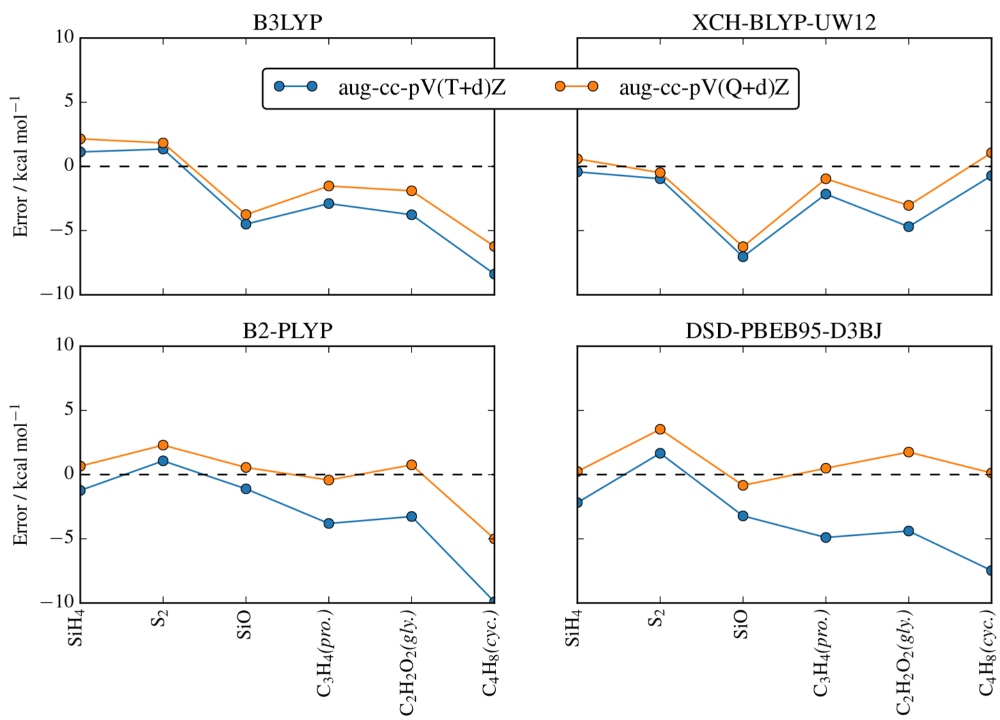

Figure 2. Atomization energy errors for individual molecules in the AE6 test set for the existing hybrid functional B3LYP,[3] the existing double-hybrid functionals B2-PLYP[14] and DSD-PBEB95-D3BJ,[46] and the new UW12 hybrid functional XCH-BLYP-UW12. The abbreviations (pro.), (gly.), and (cyc.) refer to the isomers propyne, glyoxal, and cyclobutane, respectively.

sets were performed at the geometries optimized by quadratic configuration interaction with single and double excitations with the modified Gaussian-3 basis set (QCISD/MG3).[62] Reference values (with zero-point energies removed) were taken from Tables 1 and 2 of ref 61. Individual values for all the test sets in this work are tabulated in the Supporting Information. Mean absolute errors are plotted in Figure 1, where it can be seen that $r_c = 1.7\ a_0$ (where a_0 is the Bohr radius) is around the optimum length scale for $w(r_{12})$ for both the AE6 set and the combined AE6+BH6 set, if an aug-cc-pV(Q+d)Z basis is used. In Figure 2 we plot the signed errors for individual atomization energies in the AE6 set. XCH-BLYP-UW12 converges more rapidly with respect to basis set than the existing double-hybrid functionals B2-PLYP and DSD-PBEB95-D3BJ. The slow basis-set convergence of the double hybrids is due to the double sum over unoccupied orbitals that is present in the E_c^{PT2} term. It should be noted that the parameters in B2-PLYP were optimized using a quadruple-ζ basis set. Chan and Radom[63] have investigated reoptimizing the parameters in B2-PLYP to obtain accurate results in triple-ζ basis sets, but we do not use their parameters here.

In Figure 3 we compare XCH-BLYP-UW12 (with the length scale $r_c = 1.7\ a_0$ with existing hybrid and double-hybrid functionals on larger benchmark sets of atomization energies and reaction barrier heights. The atomization-energy set referred to here as G2-1-AE-noLiBeNa contains the 49 molecules of ref 64 (G2-1 set except for the six molecules containing Li, Be, and Na), with MP2(full)/6-31G* geometries.[65] Reference values were taken from Table 2 of ref 64. The barrier-height set DBH24/08 used QCISD/MG3 geo-

DOI: 10.1021/acs.jctc.8b00337
J. Chem. Theory Comput. 2018, 14, 4590−4599

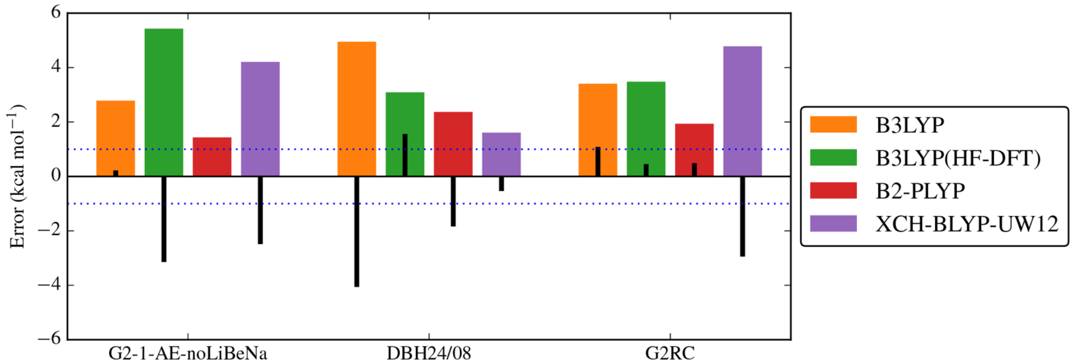

Figure 3. Root-mean-square errors (RMSEs; colored bars) and mean errors (MEs; black bars) for the larger test sets of atomization energies (G2-1-AE-noLiBeNa), reaction barrier heights (DBH24/08), and reaction energies (G2RC). HF-DFT refers to the use of density-corrected DFT (see text). Chemical accuracy (±1 kcal mol^{-1}) is shown with horizontal dotted lines. For comparison, the RMSE for the more recent double-hybrid DSD-PBEB95-D3BJ for the DBH24/08 set is 1.07 kcal mol^{-1} (taken from ref 46) and for the G2RC set is 2.33 kcal mol^{-1} (taken from ref 24).

metries.[66] Reference values were taken from Table 1 of ref 67. The aug-cc-pV(Q+d)Z basis set was used for all calculations. The zero-point energies are removed in the reference values in all cases.

Figure 3 shows that the (proof-of-concept) XCH-BLYP-UW12 functional has better accuracy than B2-PLYP for reaction barrier heights. XCH-BLYP-UW12 does not perform as well as B3LYP and B2-PLYP on the G2-1 atomization energy set, although note that this set was one of those used to fit the three parameters in B3LYP.[3,8] Note also that all of the molecules in the G2-1 atomization energy set are also in the G2/97 heats of formation set, which was used to fit the two parameters in B2-PLYP.[14] The performance demonstrated here for XCH-BLYP-UW12 is achieved with a single varied parameter, r_c, optimized over a set (AE6) of six atomization energies. Preliminary investigations suggest that performance similar to that of B2-PLYP can be achieved if two parameters are used, to adjust both the length scale r_c and the mixing of GGA and UW12.

Density-corrected[68] B3LYP—where the DFT energy is calculated using Hartree−Fock molecular orbitals—performs better than B3LYP for barrier heights, but XCH-BLYP-UW12 performs better still. XCH-BLYP-UW12 predicts barrier heights with an accuracy comparable to that of the modern DSD-PBEB95-D3BJ double hybrid (which has 6 adjustable parameters).

Reaction Energies. Results for the XCH-BLYP-UW12 functional for the G2RC[24] reaction energy test set are also plotted in Figure 3. As with the G2-1 atomization energies, we observe that XCH-BLYP-UW12 performs with roughly the same accuracy as B3LYP. Note that all the compounds in the G2RC set are also in the G2-1 and G2/97 sets.[69]

Nonbonded Interactions. Our aim in this work has been to model short-range correlation effects (since in Choosing the Geminal Operator w12 we chose $w(r_{12})$ to be a short-range function). Nevertheless, it is interesting to ask how accurate XCH-BLYP-UW12 is for modeling long-range London dispersion forces. In Figure 4 we plot the dissociation curve for the argon dimer. It is known that B2-PLYP underbinds this system, whereas MP2 overbinds. We see that XCH-BLYP-UW12 gives a binding curve that is qualitatively similar to B2-PLYP. The value of $2r_{vdW}(Ar) + r_c$ is also shown on the plot. $r_{vdW}(Ar)$ is an estimate of the van der Waals radius of the argon atom (from ref 73), so $2r_{vdW}(Ar) + r_c$ is an estimate of the bond length at which the outermost electrons on argon atom A are separated from outermost electrons on argon atom B by a distance r_c. Despite $w(r_{12})$ decaying exponentially with r_{12}, the length scale (r_c = 1.7 a_0 = 0.90 Å) is sufficiently long that XCH-BLYP-UW12 produces binding throughout the region of interest (the range of bond lengths, from 3.5 to 4.5 Å).

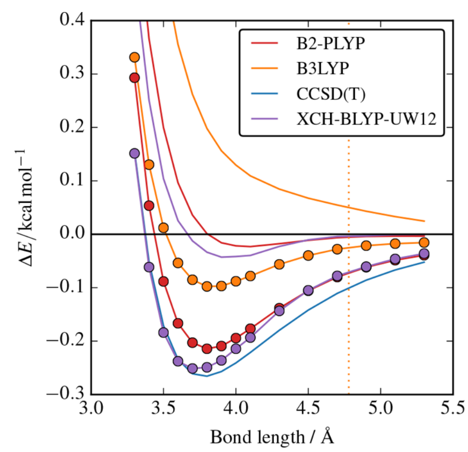

Figure 4. Dissociation curve of the argon dimer (for comparison with Figure 2 of ref 9.). Calculations used the aug-cc-pV(Q+d)Z atomic orbital basis set. For CCSD(T), a complete-basis-set (CBS) extrapolation for the quantity ΔE was used based on aug-cc-pV(T+d)Z (l_{max} = 3) values, aug-cc-pV(Q+d)Z (l_{max} = 4) values, and the formula $E(l_{max}) = E_{CBS} + Al_{max}^{-3}$. The values of A and E_{CBS} were fitted separately for each single-point energy calculation. Counterpoise correction was used for all the curves (although the same is not true for the values in Figure 2 of ref 9). Filled circles indicate the result of adding a DFT-D3BJ[70,71] empirical dispersion-correction term. The parameters for DFT-D3BJ for each functional were taken from Table S1 of the Supporting Information to ref 72. For XCH-BLYP-UW12, the same dispersion parameters were used as for B2-PLYP (without reoptimization). The frozen-core approximation was used when calculating the E_c^{PT2} term in the B2-PLYP calculations. All the electrons (both core and valence) were correlated in the XCH-BLYP-UW12 calculations. XCH-BLYP-UW12 calculations were carried out with `entos`. All other calculations (including DFT-D3BJ dispersion corrections) were calculated in Molpro. The `entos` calculations used the Def2-SVP-JKFIT density-fitting basis set. Density-fitting was not used for the Molpro calculations. The value of $2r_{vdW}(Ar) + r_c$ is shown with a vertical dotted line (see text).

DOI: 10.1021/acs.jctc.8b00337
J. Chem. Theory Comput. 2018, 14, 4590−4599

VI. CONCLUSIONS

We have shown that it is possible to define a wavefunction-like correlation model UW12 that is an explicit functional of the 1-RDM $\rho(\mathbf{x}|\mathbf{x}')$. UW12 has several advantages over the E_c^{PT2} term used in double hybrids. It has more rapid basis-set convergence and it lacks energy denominators, so divergences that can arise in PT2 are avoided and it can be included fully in the self-consistent optimization. As a result the gradient theory with respect to nuclear motions—though not developed here—is straightfoward. These advantages mean that new functionals containing UW12 may soon surpass double hybrids in terms of their applicability, performance, and computational efficiency.

We have demonstrated that the formal scaling for evaluating the UW12 energy is N^4, where N represents the size of the system. This is equivalent to the formal scaling of density-fitted Hartree–Fock exchange—a component of B3LYP. In addition, we have shown that it is possible to compute the UW12 energy and Fock matrix efficiently using ingredients (integrals and grids) that are already present in most electronic structure codes (see the Appendix).

We have suggested a one-parameter hybrid functional XCH-BLYP-UW12 containing the Unsöld correlation model, and this new functional estimates reaction barrier heights with the same level of accuracy as modern double-hybrid functionals containing six parameters. We are investigating ways to improve the performance of the method for atomization energies, while retaining the good accuracy for barrier heights, and preliminary investigations into this make us hopeful.

Our model for the geminal $w^s(r_{12})$ in eq 35 was somewhat arbitrary and based on physical intuition. In the future, we hope to fit $w^s(r_{12})$ to a model correlation system: for instance, jellium (the uniform electron gas), hookium (two electrons inside a harmonic potential well), 3-spherium (two electrons confined to the surface of a sphere in four dimensions[74]), or the helium isoelectronic series.

Further enhancements would be to replace the exchange energy $E_x = [E_x^{HF} + E_x^{B88}]/2$ with a long-range corrected exchange model, or to modify the relative scaling of the same-spin ($s = 1$) and opposite-spin ($s = 0$) components of $w^s(r_{12})$. Such enhancements have proved successful for double-hybrid functionals.[9,46,75] Using different length scales for the same-spin and opposite-spin components is another another attractive possibility when using UW12 and merits future investigation.

We conclude from this work that wavefunction-like hybrid functionals are worth further investigation. They may soon outperform double-hybrid functionals in terms of accuracy (due to orbital optimization) and in terms of computational cost (since smaller basis sets can be used).

■ APPENDIX: ALGORITHMS FOR EFFICIENT EVALUATION OF THE FOCK MATRIX

We can use density-fitting and grids to evaluate the Unsöld-W12 correlation energy (and contribution to the Fock matrix) with a computational cost that formally scales as N^4, where N is the size of the system. In this section, summation symbols are written in the positions that lead to the most efficient algorithm.

We first use density-fitting in an auxiliary basis of N_{DF} one-electron functions $\{C(\mathbf{r})\}$ to write the two-electron r_{12}^{-1} integrals as

$$\begin{aligned}\langle ij|r_{12}^{-1}|kl\rangle &\approx \sum_{CD} (ik|r_{12}^{-1}|C)(\mathbf{V}^{-1})_{CD}(D|r_{12}^{-1}|jl)\\ &= \sum_{C} (ik|r_{12}^{-1}|C)(\tilde{C}|r_{12}^{-1}|jl)\end{aligned} \tag{42}$$

where the positive-definite matrix $\mathbf{V}$ has elements $V_{DC} = (D|r_{12}^{-1}|C)$, using the notation

$$(ik|r_{12}^{-1}|C) = s_{ik}\int d\mathbf{r}_1 \int d\mathbf{r}_2\, \phi_i^*(\mathbf{r}_1)\, \phi_k(\mathbf{r}_1) r_{12}^{-1} C(\mathbf{r}_2) \tag{43}$$

$$(D|r_{12}^{-1}|C) = \int d\mathbf{r}_1 \int d\mathbf{r}_2\, D(\mathbf{r}_1) r_{12}^{-1} C(\mathbf{r}_2) \tag{44}$$

We express the two-electron $w(r_{12})$ integrals on a grid as

$$\langle ij|w_{12}|kl\rangle = \sum_{\lambda} w_\lambda \phi_j^*(\mathbf{r}_\lambda)\, \phi_l(\mathbf{r}_\lambda)\, s_{jl}(\mathbf{r}_\lambda|w_{12}^{s_{ij}}|ik) \tag{45}$$

where $(\mathbf{r}_\lambda|w_{12}|\beta j) = \langle\beta|w(\mathbf{r}-\mathbf{r}_\lambda)|j\rangle$, and where λ refers to a grid point at position $\mathbf{r}_\lambda$ with grid weight w_λ.

In this section, we separate the direct ($+$, $|\overline{pq}\rangle = |pq\rangle$) and indirect ($-$, $|\overline{pq}\rangle = -|qp\rangle$) components of E_c^{UW12} such that

$$E_{c,2el}^{UW12} = E_{c,2el,+}^{UW12} + E_{c,2el,-}^{UW12} \tag{46}$$

$$E_{c,3el}^{UW12} = E_{c,3el,+}^{UW12} + E_{c,3el,-}^{UW12} \tag{47}$$

$$E_{c,4el}^{UW12} = E_{c,4el,+}^{UW12} + E_{c,4el,-}^{UW12} \tag{48}$$

Substituting eqs 40, 42, and 45 into eqs 19, 21, and 20, and differentiating with respect to the elements $D_{\alpha\beta}^{\sigma}$ of the density matrix in the atomic-orbital basis we obtain the contributions to the Fock matrix

$$\begin{aligned}\frac{\partial E_{c,2el,+}^{UW12}}{\partial D_{\alpha\beta}^{\sigma}} &= \sum_j \langle\alpha j|w_{12}r_{12}^{-1}|\beta j\rangle\\ &= \sum_\lambda w_\lambda \alpha^*(\mathbf{r}_\lambda) \sum_j (\mathbf{r}_\lambda|w_{12}^{\delta_{\sigma_j\sigma}} r_{12}^{-1}|jj)\beta(\mathbf{r}_\lambda)\end{aligned} \tag{49}$$

$$\begin{aligned}\frac{\partial E_{c,2el,-}^{UW12}}{\partial D_{\alpha\beta}^{\sigma}} &= -\sum_j \delta_{\sigma_j\sigma}\langle j\alpha|w_{12}r_{12}^{-1}|\beta j\rangle\\ &= -\sum_\lambda w_\lambda \alpha^*(\mathbf{r}_\lambda) \sum_j \delta_{\sigma_j\sigma}\phi_j^*(\mathbf{r}_\lambda)(\mathbf{r}_1|w_{12}^{1}r_{12}^{-1}|\beta j)\end{aligned} \tag{50}$$

$$\begin{aligned}\frac{\partial E_{c,3el,+}^{UW12}}{\partial D_{\alpha\beta}^{\sigma}} &= -2\sum_{jk} \langle\alpha jk|w_{12}r_{23}^{-1}|kj\beta\rangle - \sum_{jk}\langle j\alpha k|w_{12}r_{23}^{-1}|k\beta j\rangle\\ &= -2\sum_\lambda w_\lambda\left[\sum_j \phi_j^*(\mathbf{r}_\lambda)\,\phi_j(\mathbf{r}_\lambda)\right]\left[\sum_k \delta_{\sigma_k\sigma}(\mathbf{r}_\lambda|w_{12}^{\delta_{\sigma_j\sigma}}|\alpha k)(\mathbf{r}_\lambda|r_{12}^{-1}|k\beta)\right]\\ &\quad - \sum_\lambda w_\lambda[\alpha^*(\mathbf{r}_\lambda)\,\beta(\mathbf{r}_\lambda)]\left[\sum_{jk}(\mathbf{r}_\lambda|w_{12}^{\delta_{\sigma_j\sigma}}|jk)(\mathbf{r}_\lambda|r_{12}^{-1}|kj)\right]\end{aligned} \tag{51}$$

DOI: 10.1021/acs.jctc.8b00337
J. Chem. Theory Comput. 2018, 14, 4590–4599

$$
\begin{aligned}
\frac{\partial E_{\mathrm{c,3el,-}}^{\mathrm{UW12}}}{\partial D_{\alpha\beta}^{\sigma}} &= \sum_{jk} \langle j\alpha k|w_{12}r_{23}^{-1}|kj\beta\rangle + \sum_{jk} \langle \alpha jk|w_{12}r_{23}^{-1}|k\beta j\rangle \\
&\quad + \sum_{jk} \langle jk\alpha|w_{12}r_{23}^{-1}|\beta jk\rangle \\
&= \sum_{\lambda} w_{\lambda}[\alpha^{*}(\mathbf{r}_{\lambda})]\left[\sum_{j} \delta_{\sigma_j\sigma}\phi_j(\mathbf{r}_{\lambda}) \sum_{k} (\mathbf{r}_{\lambda}|w_{12}^{1}|jk)(\mathbf{r}_{\lambda}|r_{12}^{-1}|k\beta)\right] \\
&\quad + \sum_{\lambda} w_{\lambda}[\beta(\mathbf{r}_{\lambda})]\left[\sum_{j} \phi_j^{*}(\mathbf{r}_{\lambda})\delta_{\sigma_j\sigma} \sum_{k} (\mathbf{r}_{\lambda}|w_{12}^{1}|\alpha k)(\mathbf{r}_{\lambda}|r_{12}^{-1}|kj)\right] \\
&\quad + \sum_{\lambda} w_{\lambda}\left[\sum_{j} \phi_j(\mathbf{r}_{\lambda})(\mathbf{r}_{\lambda}|w_{12}^{1}|j\beta)\right]\left[\sum_{k} \phi_k^{*}(\mathbf{r}_{\lambda})(\mathbf{r}_{\lambda}|r_{12}^{-1}|\alpha k)\right]
\end{aligned} \tag{52}
$$

$$
\begin{aligned}
\frac{\partial E_{\mathrm{c,4el,+}}^{\mathrm{UW12}}}{\partial D_{\alpha\beta}^{\sigma}} &= 2\sum_{jkl} \langle \alpha j|w_{12}|kl\rangle\langle kl|r_{12}^{-1}|\beta j\rangle \\
&= 2\sum_{\lambda} w_{\lambda}\alpha^{*}(\mathbf{r}_{\lambda}) \sum_{C}\left[\sum_{jl} (\mathbf{r}_{\lambda}|w_{12}^{\delta_{\sigma_j\sigma}}|jl)(\tilde{C}|r_{12}^{-1}|lj)\right] \\
&\quad \times \left[\sum_{k} \delta_{\sigma_k\sigma}\phi_k(\mathbf{r}_{\lambda})(k\beta|r_{12}^{-1}|C)\right]
\end{aligned} \tag{53}
$$

$$
\begin{aligned}
\frac{\partial E_{\mathrm{c,4el,-}}^{\mathrm{UW12}}}{\partial D_{\alpha\beta}^{\sigma}} &= -2\sum_{jkl} \delta_{\sigma_j\sigma}\langle \alpha j|w_{12}|kl\rangle\langle lk|r_{12}^{-1}|\beta j\rangle \\
&= -2\sum_{\lambda} w_{\lambda}\alpha^{*}(\mathbf{r}_{\lambda}) \sum_{Cl} (l\beta|r_{12}^{-1}|C) \sum_{j} (\mathbf{r}_{\lambda}|w_{12}^{1}|jl) \\
&\quad \times \sum_{k} \delta_{\sigma_k\sigma}\phi_k(\mathbf{r}_{\lambda})(\tilde{C}|r_{12}^{-1}|kj)
\end{aligned} \tag{54}
$$

In this form, we observe that the computational scaling[76] of evaluating $\partial E_{\mathrm{c}}^{\mathrm{UW12}}/\partial D_{\alpha\beta}^{\sigma}$ will be $N_{\mathrm{AO}}N_{\mathrm{DF}}N_{\mathrm{grid}}N_{\mathrm{el}}$. To see this, consider the number of terms in (for instance) the summation over C and l in eq 54. N_{AO}, N_{DF}, N_{grid}, and N_{el} all scale linearly with the system size N.

As a final remark, we note that one may use standard screening and molecular-orbital localization and exploit the short-range nature of the geminal function $w(r_{12})$ to reduce the scaling further.[77]

■ ASSOCIATED CONTENT

Supporting Information

The Supporting Information is available free of charge on the ACS Publications website at DOI: 10.1021/acs.jctc.8b00337.

Tables of coefficients $c_{s\gamma}$ used in eq 38 and tables of individual atomization energies and barrier heights for the test sets mentioned in the text (PDF)

■ AUTHOR INFORMATION

Corresponding Author

*E-mail: fred.manby@bristol.ac.uk.

ORCID

Frederick R. Manby: 0000-0001-7611-714X

Notes

The authors declare no competing financial interest.

All data from this work are held in an open-access repository that can be accessed at https://data.bris.ac.uk/data/dataset/fxmuvujgeid2css1z2krpe3o.

■ ACKNOWLEDGMENTS

We thank David Tew for numerous helpful discussions. T.C.W. is funded through the Engineering and Physical Sciences Research Council (EPSRC) Centre for Doctoral Training in Theory and Modelling in Chemical Sciences (Grant EPSRC EP/L015722/1).

■ REFERENCES

(1) A "semi-local" functional $E[\rho]$ depends only on the electron (spin-)density $\rho^{\sigma}(\mathbf{r})$ at point $\mathbf{r}$ and on derivative quantities at point $\mathbf{r}$.

(2) We use $\mathbf{x}$ to refer to both space ($\mathbf{r}$) and spin (σ) coordinates.

(3) Becke, A. D. Density-functional thermochemistry. III. The role of exact exchange. *J. Chem. Phys.* **1993**, *98*, 5648−5652. Note: There are multiple variants of the VWN functional presented in ref 4. The most commonly used in quantum chemistry are known as VWN(III) and VWN(V). These are used to construct two variants of B3LYP: known as B3LYP3 and B3LYP5. We choose to use B3LYP3 throughout for compatibility with ref 11. All references to B3LYP thus refer to B3LYP3 instead of B3LYP5.

(4) Vosko, S. H.; Wilk, L.; Nusair, M. Accurate spin-dependent electron liquid correlation energies for local spin density calculations: a critical analysis. *Can. J. Phys.* **1980**, *58*, 1200−1211.

(5) Lee, C.; Yang, W.; Parr, R. G. Development of the Colle-Salvetti correlation-energy formula into a functional of the electron density. *Phys. Rev. B: Condens. Matter Mater. Phys.* **1988**, *37*, 785−789.

(6) Becke, A. D. Density-functional exchange-energy approximation with correct asymptotic behavior. *Phys. Rev. A: At., Mol., Opt. Phys.* **1988**, *38*, 3098−3100.

(7) To fit the parameters in B3LYP, the energy components in eq 4 were evaluated using the Kohn−Sham orbitals from a previous self-consistent LDA calculation.[3]

(8) Gill, P. M. W.; Johnson, B. G.; Pople, J. A.; Frisch, M. J. An investigation of the performance of a hybrid of Hartree-Fock and density functional theory. *Int. J. Quantum Chem.* **1992**, *44*, 319−331.

(9) Goerigk, L.; Grimme, S. Double-hybrid density functionals. *WIREs Comput. Mol. Sci.* **2014**, *4*, 576−600.

(10) Becke, A. D. A new mixing of Hartree-Fock and local density-functional theories. *J. Chem. Phys.* **1993**, *98*, 1372−1377.

(11) Sharkas, K.; Toulouse, J.; Savin, A. Double-hybrid density-functional theory made rigorous. *J. Chem. Phys.* **2011**, *134*, 064113.

(12) It should be noted that many more recent hybrid functionals achieve this, albeit at the expense of having many more tunable parameters than B3LYP. M05-2X[78] and ωB97X-V[79] are examples of hybrid functionals that perform well for atomization energies and barrier heights but have many tunable parameters (M05-2X has 20 tunable parameters, and ωB97X-V has 10, compared to B3LYP which has 3). Our aim in this work is to search for new ingredients to add to hybrid DFT in such a way that the number of tunable parameters remains low.

(13) Another motivating factor for adding nonlocal correlation terms to the energy expression is that hybrid DFT functionals perform poorly for many classes of noncovalent interactions between molecules (even when an empirical dispersion correction term is added). This is true even of the most recent hybrid functionals.[23]

(14) Grimme, S. Semiempirical hybrid density functional with perturbative second-order correlation. *J. Chem. Phys.* **2006**, *124*, 034108.

(15) Görling, A.; Levy, M. Correlation-energy functional and its high-density limit obtained from a coupling-constant perturbation expansion. *Phys. Rev. B: Condens. Matter Mater. Phys.* **1993**, *47*, 13105−13113.

(16) Görling, A.; Levy, M. Exact Kohn-Sham scheme based on perturbation theory. *Phys. Rev. A: At., Mol., Opt. Phys.* **1994**, *50*, 196−204.

(17) Zhao, Y.; Lynch, B. J.; Truhlar, D. G. Doubly Hybrid Meta DFT: New Multi-Coefficient Correlation and Density Functional Methods for Thermochemistry and Thermochemical Kinetics. *J. Phys. Chem. A* **2004**, *108*, 4786−4791.

(18) Zhao, Y.; Lynch, B. J.; Truhlar, D. G. Multi-coefficient extrapolated density functional theory for thermochemistry and thermochemical kinetics. *Phys. Chem. Chem. Phys.* **2005**, *7*, 43−52.
(19) Toulouse, J.; Sharkas, K.; Brémond, E.; Adamo, C. Communication: Rationale for a new class of double-hybrid approximations in density-functional theory. *J. Chem. Phys.* **2011**, *135*, 101102.
(20) Such double-hybrid functionals are sometimes referred to as "truncated", since the orbitals are optimized using a part of the full energy expression.
(21) Zhang, Y.; Xu, X.; Goddard, W. A. Doubly hybrid density functional for accurate descriptions of nonbond interactions, thermochemistry, and thermochemical kinetics. *Proc. Natl. Acad. Sci. U. S. A.* **2009**, *106*, 4963−4968.
(22) Su, N. Q.; Yang, W.; Mori-Sánchez, P.; Xu, X. Fractional Charge Behavior and Band Gap Predictions with the XYG3 Type of Doubly Hybrid Density Functionals. *J. Phys. Chem. A* **2014**, *118*, 9201−9211.
(23) Mardirossian, N.; Head-Gordon, M. Thirty years of density functional theory in computational chemistry: an overview and extensive assessment of 200 density functionals. *Mol. Phys.* **2017**, *115*, 2315−2372.
(24) Goerigk, L.; Hansen, A.; Bauer, C.; Ehrlich, S.; Najibi, A.; Grimme, S. A look at the density functional theory zoo with the advanced GMTKN55 database for general main group thermochemistry, kinetics and noncovalent interactions. *Phys. Chem. Chem. Phys.* **2017**, *19*, 32184−32215.
(25) Wang, J.; Liu, L.; Wilson, A. K. Oxidative Cleavage of the β-O-4 Linkage of Lignin by Transition Metals: Catalytic Properties and the Performance of Density Functionals. *J. Phys. Chem. A* **2016**, *120*, 737−746.
(26) Verma, P.; Varga, Z.; Klein, J. E. M. N.; Cramer, C. J.; Que, L.; Truhlar, D. G. Assessment of electronic structure methods for the determination of the ground spin states of Fe(ii), Fe(iii) and Fe(iv) complexes. *Phys. Chem. Chem. Phys.* **2017**, *19*, 13049−13069.
(27) Kurlancheek, W.; Head-Gordon, M. Violations of N-representability from spin-unrestricted orbitals in Møller-Plesset perturbation theory and related double-hybrid density functional theory. *Mol. Phys.* **2009**, *107*, 1223−1232.
(28) Lochan, R. C.; Head-Gordon, M. Orbital-optimized opposite-spin scaled second-order correlation: An economical method to improve the description of open-shell molecules. *J. Chem. Phys.* **2007**, *126*, 164101.
(29) Neese, F.; Schwabe, T.; Kossmann, S.; Schirmer, B.; Grimme, S. Assessment of Orbital-Optimized, Spin-Component Scaled Second-Order Many-Body Perturbation Theory for Thermochemistry and Kinetics. *J. Chem. Theory Comput.* **2009**, *5*, 3060−3073.
(30) Peverati, R.; Head-Gordon, M. Orbital optimized double-hybrid density functionals. *J. Chem. Phys.* **2013**, *139*, 024110.
(31) Sancho-García, J. C.; Pérez-Jiménez, A. J.; Savarese, M.; Brémond, E.; Adamo, C. Importance of Orbital Optimization for Double-Hybrid Density Functionals: Application of the OO-PBE-QIDH Model for Closed- and Open-Shell Systems. *J. Phys. Chem. A* **2016**, *120*, 1756−1762.
(32) Śmiga, S.; Franck, O.; Mussard, B.; Buksztel, A.; Grabowski, I.; Luppi, E.; Toulouse, J. Self-consistent double-hybrid density-functional theory using the optimized-effective-potential method. *J. Chem. Phys.* **2016**, *145*, 144102.
(33) Jin, Y.; Zhang, D.; Chen, Z.; Su, N. Q.; Yang, W. Generalized Optimized Effective Potential for Orbital Functionals and Self-Consistent Calculation of Random Phase Approximations. *J. Phys. Chem. Lett.* **2017**, *8*, 4746−4751.
(34) Note that singly excited determinants are ignored in this theory and are probably mainly accounted for through orbital optimization. Single excitations are also often ignored in double hybrid, even without orbital optimization.[9,14]
(35) Werner, H.-J.; Adler, T. B.; Manby, F. R. General orbital invariant MP2-F12 theory. *J. Chem. Phys.* **2007**, *126*, 164102.
(36) Adler, T. B.; Knizia, G.; Werner, H.-J. A simple and efficient CCSD(T)-F12 approximation. *J. Chem. Phys.* **2007**, *127*, 221106.
(37) Grüneis, A. Efficient Explicitly Correlated Many-Electron Perturbation Theory for Solids: Application to the Schottky Defect in MgO. *Phys. Rev. Lett.* **2015**, *115*, 066402.
(38) Häser, M.; Almlöf, J. Laplace transform techniques in Møller-Plesset perturbation theory. *J. Chem. Phys.* **1992**, *96*, 489−494.
(39) Klopper, W.; Manby, F. R.; Ten-No, S.; Valeev, E. F. R12 methods in explicitly correlated molecular electronic structure theory. *Int. Rev. Phys. Chem.* **2006**, *25*, 427−468.
(40) Kong, L.; Bischoff, F. A.; Valeev, E. F. Explicitly Correlated R12/F12 Methods for Electronic Structure. *Chem. Rev.* **2012**, *112*, 75−107.
(41) Ten-no, S. Initiation of explicitly correlated Slater-type geminal theory. *Chem. Phys. Lett.* **2004**, *398*, 56−61.
(42) Our aim in this work is to demonstrate a hybrid functional which gives (roughly) the same results as B2-PLYP, but while only using occupied Kohn−Sham orbitals. Hence we choose a_x^{HF}, $a_c^{\mathrm{LYP}} = 1$, $(1 - \lambda^2) = \frac{1}{2}, \frac{3}{4}$ to enable direct comparisons with B2-PLYP (which has a_x^{HF}, $a_c^{\mathrm{LYP}} = 0.53, 0.73$). Developers of double-hybrid functionals[46] have found that it is possible to construct functionals with comparable accuracy for a range of values of a_x^{HF} (in the range 0.45−0.75), and we expect the same to be true of our XCH functionals. In future, we intend to publish results using a range of values of a_x^{HF}.
(43) Boys, S. F.; Handy, N. C. The Determination of Energies and Wavefunctions with Full Electronic Correlation. *Proc. R. Soc. London, Ser. A* **1969**, *310*, 43−61.
(44) Ten-no, S. Explicitly correlated second order perturbation theory: Introduction of a rational generator and numerical quadratures. *J. Chem. Phys.* **2004**, *121*, 117−129.
(45) Gill, P. M.; Johnson, B. G.; Pople, J. A. A standard grid for density functional calculations. *Chem. Phys. Lett.* **1993**, *209*, 506−512.
(46) Kozuch, S.; Martin, J. M. L. Spin-component-scaled double hybrids: An extensive search for the best fifth-rung functionals blending DFT and perturbation theory. *J. Comput. Chem.* **2013**, *34*, 2327−2344.
(47) Goerigk, L.; Grimme, S. Efficient and Accurate Double-Hybrid-Meta-GGA Density Functionals−Evaluation with the Extended GMTKN30 Database for General Main Group Thermochemistry, Kinetics, and Noncovalent Interactions. *J. Chem. Theory Comput.* **2011**, *7*, 291−309.
(48) Zhang, I. Y.; Xu, X.; Jung, Y.; Goddard, W. A. A fast doubly hybrid density functional method close to chemical accuracy using a local opposite spin ansatz. *Proc. Natl. Acad. Sci. U. S. A.* **2011**, *108*, 19896−19900.
(49) Benighaus, T.; DiStasio, R. A.; Lochan, R. C.; Chai, J.-D.; Head-Gordon, M. Semiempirical Double-Hybrid Density Functional with Improved Description of Long-Range Correlation. *J. Phys. Chem. A* **2008**, *112*, 2702−2712.
(50) Manby, F. R., Miller, T. F., III *entos*, an electronic structure program; 2017.
(51) Dunning, T. H., Jr. Gaussian basis sets for use in correlated molecular calculations. I. The atoms boron through neon and hydrogen. *J. Chem. Phys.* **1989**, *90*, 1007−1023.
(52) Kendall, R. A.; Dunning, T. H., Jr.; Harrison, R. J. Electron affinities of the first-row atoms revisited Systematic basis sets and wave functions. *J. Chem. Phys.* **1992**, *96*, 6796−6806.
(53) Woon, D. E.; Dunning, T. H., Jr. Gaussian basis sets for use in correlated molecular calculations. III. The atoms aluminum through argon. *J. Chem. Phys.* **1993**, *98*, 1358−1371.
(54) Woon, D. E.; Dunning, T. H., Jr. Gaussian basis sets for use in correlated molecular calculations. IV Calculation of static electrical response properties. *J. Chem. Phys.* **1994**, *100*, 2975−2988.
(55) Dunning, T. H., Jr.; Peterson, K. A.; Wilson, A. K. Gaussian basis sets for use in correlated molecular calculations. X. The atoms aluminum through argon revisited. *J. Chem. Phys.* **2001**, *114*, 9244−9253.
(56) This is in keeping with the original B2-PLYP publication.[14] The authors of ref 46 ran similar calculations both with and without the

frozen-core approximation and found that there was little difference in the performance (provided the parameters were reoptimized in each case).

(57) Werner, H.-J.; Knowles, P. J.; Knizia, G.; Manby, F. R.; Schütz, M.; et al. *MOLPRO*, version 2015.1, a package of ab initio programs; 2015; http://www.molpro.net.

(58) Werner, H.-J.; Knowles, P. J.; Knizia, G.; Manby, F. R.; Schütz, M. Molpro: a general-purpose quantum chemistry program package. *WIREs Comput. Mol. Sci.* **2012**, *2*, 242−253.

(59) Weigend, F.; Ahlrichs, R. Balanced basis sets of split valence, triple zeta valence and quadruple zeta valence quality for H to Rn: Design and assessment of accuracy. *Phys. Chem. Chem. Phys.* **2005**, *7*, 3297−3305.

(60) Weigend, F. Hartree-Fock exchange fitting basis sets for H to Rn. *J. Comput. Chem.* **2008**, *29*, 167−175.

(61) Lynch, B. J.; Truhlar, D. G. Small Representative Benchmarks for Thermochemical Calculations. *J. Phys. Chem. A* **2003**, *107*, 8996−8999.

(62) QCISD/MG3 geometries for AE6 and BH6 compounds were taken from the Minnesota Database Collection at https://comp.chem.umn.edu/db/.

(63) Chan, B.; Radom, L. Obtaining Good Performance With Triple-ζ-Type Basis Sets in Double-Hybrid Density Functional Theory Procedures. *J. Chem. Theory Comput.* **2011**, *7*, 2852−2863.

(64) Fast, P. L.; Corchado, J.; Sanchez, M. L.; Truhlar, D. G. Optimized Parameters for Scaling Correlation Energy. *J. Phys. Chem. A* **1999**, *103*, 3139−3143.

(65) MP2(full)/6-31G* geometries were obtained from the Argonne National Laboratory Web site http://www.cse.anl.gov/OldCHMwebsiteContent/compmat/g2geoma.htm.

(66) QCISD/MG3 geometries for DBH24/08 compounds were taken from the Minnesota Database Collection at http://comp.chem.umn.edu/db/.

(67) Zheng, J.; Zhao, Y.; Truhlar, D. G. The DBH24/08 Database and Its Use to Assess Electronic Structure Model Chemistries for Chemical Reaction Barrier Heights. *J. Chem. Theory Comput.* **2009**, *5*, 808−821.

(68) Kim, M.-C.; Sim, E.; Burke, K. Understanding and Reducing Errors in Density Functional Calculations. *Phys. Rev. Lett.* **2013**, *111*, 073003.

(69) MP2(full)/6-31G(d) geometries and reference values (with single-point energies removed) are taken from the GMTKN55 database collection at http://www.chemie.uni-bonn.de/pctc/mulliken-center/software/GMTKN/gmtkn55/.

(70) Grimme, S.; Antony, J.; Ehrlich, S.; Krieg, H. A consistent and accurate ab initio parametrization of density functional dispersion correction (DFT-D) for the 94 elements H-Pu. *J. Chem. Phys.* **2010**, *132*, 154104.

(71) Grimme, S.; Ehrlich, S.; Goerigk, L. Effect of the damping function in dispersion corrected density functional theory. *J. Comput. Chem.* **2011**, *32*, 1456−1465.

(72) Goerigk, L.; Grimme, S. A thorough benchmark of density functional methods for general main group thermochemistry, kinetics, and noncovalent interactions. *Phys. Chem. Chem. Phys.* **2011**, *13*, 6670−6688.

(73) Vogt, J.; Alvarez, S. van der Waals Radii of Noble Gases. *Inorg. Chem.* **2014**, *53*, 9260−9266.

(74) Loos, P.-F.; Gill, P. M. Excited states of spherium. *Mol. Phys.* **2010**, *108*, 2527−2532.

(75) Chai, J.-D.; Head-Gordon, M. Long-range corrected double-hybrid density functionals. *J. Chem. Phys.* **2009**, *131*, 174105.

(76) In estimating the slowest step of the calculation, we assume that $N_{grid} > N_{DF} > N_{AO} > N_{el}$.

(77) For a helpful introduction to some of the techniques that can be used to reduce the computational expense (both scaling and prefactor) of MP2-like correlation models, see the section labeled "Summary of local OS PT2 approximations" in the Supporting Information of ref 48.

(78) Zhao, Y.; Schultz, N. E.; Truhlar, D. G. Design of Density Functionals by Combining the Method of Constraint Satisfaction with Parametrization for Thermochemistry, Thermochemical Kinetics, and Noncovalent Interactions. *J. Chem. Theory Comput.* **2006**, *2*, 364−382.

(79) Mardirossian, N.; Head-Gordon, M. wB97X-V: A 10-parameter, range-separated hybrid, generalized gradient approximation density functional with nonlocal correlation, designed by a survival-of-the-fittest strategy. *Phys. Chem. Chem. Phys.* **2014**, *16*, 9904−9924.

DOI: 10.1021/acs.jctc.8b00337
J. Chem. Theory Comput. 2018, 14, 4590−4599